http://dx.doi.org/10.5516/NET.09.2014.030

PROBABILISTIC SEISMIC ASSESSMENT OF BASE-ISOLATED NPPS SUBJECTED TO STRONG GROUND MOTIONS OF TOHOKU EARTHQUAKE

AHMER ALI[1], NADIN ABU HAYAH[1], DOOKIE KIM[1*], and SUNG GOOK CHO[2]
[1]Department of Civil and Environmental Engineering, Kunsan National University, Jeonbuk, Korea
[2]R & D Center, JACE KOREA Company, Gyeonggi-do, Korea
[*]Corresponding author. E-mail : kim2kie@kunsan.ac.kr

Received March 19, 2014
Accepted for Publication June 13, 2014

The probabilistic seismic performance of a standard Korean nuclear power plant (NPP) with an idealized isolation is investigated in the present work. A probabilistic seismic hazard analysis (PSHA) of the Wolsong site on the Korean peninsula is performed by considering peak ground acceleration (PGA) as an earthquake intensity measure. A procedure is reported on the categorization and selection of two sets of ground motions of the Tohoku earthquake, i.e. long-period and common as *Set A* and *Set B* respectively, for the nonlinear time history response analysis of the base-isolated NPP. Limit state values as multiples of the displacement responses of the NPP base isolation are considered for the fragility estimation. The seismic risk of the NPP is further assessed by incorporation of the rate of frequency exceedance and conditional failure probability curves. Furthermore, this framework attempts to show the unacceptable performance of the isolated NPP in terms of the probabilistic distribution and annual probability of limit states. The comparative results for long and common ground motions are discussed to contribute to the future safety of nuclear facilities against drastic events like Tohoku.

KEYWORDS : Probabilistic Risk and Hazard Assessment; Ground Motion Selection; Long-period Ground Motions; Seismic Isolation; Nuclear Power Plant

1. INTRODUCTION

In earthquake engineering, probabilistic seismic hazard assessment (PSHA) efficiently determines the ground motion intensity corresponding to the target hazard level, i.e. annual probability of intensity exceedance. In that regard, Nakajima *et al*. evaluated the seismic hazard for eight sites in Korea with PGA and spectral acceleration as indices of seismic motions, and studied the regional difference in the hazard levels of the Korean sites [1]. Later, Choi *et al*. developed site-specific uniform hazard spectra (UHS) for Korean NPP sites using four seismic source models. The parametric dominancy of earthquakes has affected the shape of UHS and hence, different hazard curves were found for four sites as a different attenuation relation was used for each target site [2].

Since the hazard curve provides useful information about the intensity measurement of a ground motion, it can be utilized in conducting the studies on probabilistic seismic risk assessment (PSRA). In this PSRA framework, state of the art research on the computation of the seismic fragility of NPP components has been performed by Kennedy *et al*. [3]. The study mainly dealt with the probabilistic seismic safety evaluation of an existing nuclear power plant. A methodology was presented to develop the NPP structure and equipment fragility curves as a function of the peak ground acceleration. Later, as the part of the overall work, a procedure on the estimation of component seismic fragility and their use in probabilistic risk assessment (PRA) was reported by Kennedy and Ravindra [4]. Zentner statistically estimated the parameters of fragility curves for the NPP reactor coolant system by means of Monte-Carlo simulation. The numerical simulation involved the nonlinear dynamic response analyses using artificial time histories and accounts for the propagation of uncertainties due to seismic loads [5]. Pisharady and Basu outlined a brief summary of the different methods to derive the seismic fragility of NPP components. The approaches emphasized the determination of factors relevant to strength, capacity and seismic demand. The study also reports the estimation of overall and global NPP structure, system or component (SSC) fragility using fragility of different failure modes and element fragility [6].

The interpretation of seismic vulnerability of isolated NPPs by risk analysis and fragility curves has been practiced for decades. All over the world, a rise in the risk and safety concerns of nuclear facilities has been noticed since the devastating Tohoku earthquake and the consequential instabilities to the Japanese NPPs. The event had relatively long-period (1 to 10sec or longer) ground motions with low-frequency shakes; much more than the short period

(1sec or shorter) ground motions. The lateral force-resisting systems of structures with long fundamental period being more susceptible to low-frequency long duration seismic signals have been witnessed to be substantially affected in Japan. Therefore, the significance and use of long-period motions in risk and safety studies has received prime attention from researchers in the field of nuclear and earthquake engineering. Furumura *et al*. Reported the significance of the anomalous strong ground motions of the Tohoku earthquake (M=9.0) by comparing the associated high-frequency content and long-period character with past destructive events like the 1995 Kobe earthquake (M=7.3), the 2004 SE Off-Kii Peninsula earthquake (M=7.4), the 2004 Mid-Niigata earthquake (M=6.8), and the 1994 Tonankai earthquake (M=8) [7]. Tkewaki, and Tkewaki *et al*. investigated the response attributes of tall buildings by their resonance under the critical impact of the long-period ground motion records of the Tohoku earthquake. The presence of an appreciably higher long-period wave component in the records was verified by observing the velocity and earthquake input energy spectra. Moreover, the use of high-hardness rubber dampers served efficiently against the associated vibrations in shorter durations as compared to the buildings with no damping [8, 9]. Xiang and Li suggested a study on long-period response spectra as a reference for the seismic design code revision of building structures in China. The long-period ground motions were recorded in the US and analyzed by the authors. The corner periods of the spectra were statistically determined corresponding to the Chinese design spectrum, whereas the associated horizontal motions were grouped by means of site categorization [10].

This study focuses on the probabilistic seismic evaluation of base isolated NPPs subjected to the strong ground motions of the Tohoku earthquake. The two groups of seismic inputs for time history analyses, named as *Set A* and *Set B* (i.e. common and long-period), are selected with the spectral compatibility of the NRC target spectra. The probable failure of the NPP is evaluated by means of fragility curves. Moreover, the probabilistic unacceptable performance of the NPP is assessed by adjoining the risk analysis results with the seismic hazard curve of a Korean site source model. The results are taken under discussion to demonstrate the substantially significant impact of long-period ground motions.

2. NPP STRUCTURAL AND STICK MODEL

2.1 FE Stick Model

For the time history analyses, the lumped mass structural stick model of a standard Korean NPP containment building is developed in the OpenSees platform [11]. The model is 65.84 *m* high and it contains 15 nodes and 14 elements. The first 13 elastic beam-column elements (i.e. elements No. 2 to 14) deploy the sectional properties of the reactor building with the details of concentrated mass at each node and the moment of inertia of each element is shown in table 1 [12]. The LRB is further modeled using a special "elastomeric Bearing" element object in Open-

Table 1. Nodal Mass & Element Stiffness Details of Base-Isolated NPP Reactor Building

Node No.	Elevation (m)	Translation Mass ($kN.s^2/m$)	Rotational Mass ($\times 10^4$ kN.m.s^2)		Element No.	Geometric Moment of Inertia ($\times 10^4$ m^4)	Polar Moment of Inertia ($\times 10^4$ m^4)
		X=Y=Z	XX=YY	ZZ			
1	0.000	-	-	-	1	-	-
2	0.000	1074.058	27.417	54.832	2	4.398	8.795
3	5.182	1914.917	48.110	95.494	3	4.398	8.795
4	8.534	1390.876	35.435	70.870	4	4.398	8.795
5	11.89	1648.591	36.519	75.865	5	4.398	8.795
6	14.94	1264.499	32.208	64.417	6	4.398	8.795
7	17.98	1328.563	41.545	87.118	7	4.398	8.795
8	21.34	2086.095	53.250	10.650	8	4.398	8.795
9	28.04	3603.493	92.379	18.476	9	4.398	8.795
10	38.71	2844.794	72.950	14.590	10	4.398	8.795
11	41.76	2004.081	40.060	82.248	11	4.398	8.795
12	44.81	2009.918	49.893	98.454	12	3.753	7.506
13	52.43	2756.359	62.581	12.249	13	2.856	5.713
14	60.05	2756.359	39.340	75.932	14	1.152	23.04
15	65.84	1241.733	5.8605	11.371	-	-	-

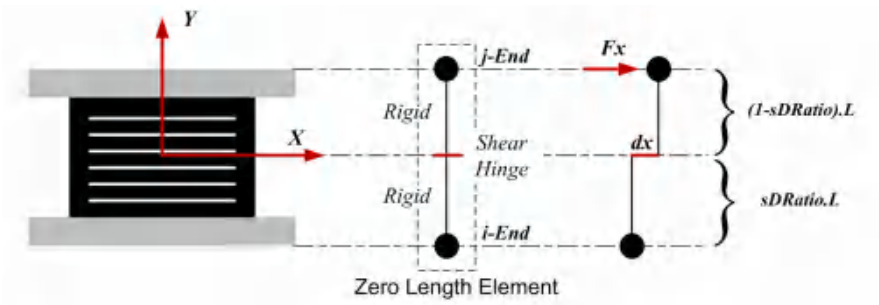

Fig. 1. Zero-length ElastomericBearing Element in OpenSees

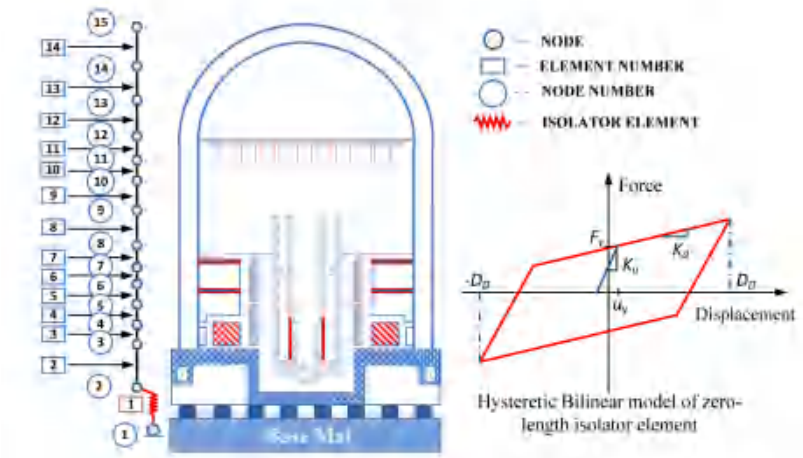

Fig. 2. Structural Stick Model of Standard Korean NPP with Idealized Bilinear Hysteretic Isolator

Sees which can be used in conjunction with a zero-length isolator element (i.e. element No. 1) or an element with an appropriate bearing height. The behavioral mechanics of a zero-length elastomeric element is sketched in Figure 1, where *sDRatio* refers to the shear distance from the *i*-end of the element as a fraction of element length *L*. In the present study, the shear hinge is located at the center of the element, i.e. *sDRatio*=0. 5, so that the P-delta moments can be equally distributed to both end nodes.

A constitutive model entailing bilinear hysteretic properties is used and assigned to the bearing element to reflect the shear and force deformation material behavior. Figure 2 shows the finite element NPP model configured with the bilinear LRB isolator element. The primitive validation of the complete FE model is done by performing modal analysis; acquiring 2.54 sec as a fundamental period to match the designed target period, i.e. 2.5 sec.

The physical characteristics of the LRB isolator are obtained from the experimental test studies conducted by UNISON in collaboration with the Korea Testing and Research Institute (KTRI), and so designed by the guidelines provided by Naeim and Kelly [13, 14]. The specifications of ISO 22762:2010, 6.2.2 were followed to perform the compression-shear test with the test apparatus shown in Figure 3 [15]. The horizontal and vertical load capacity parameters of the testing equipment are illustrated in table 2.

Fig. 3. Compression-Shear Load Tester

Table 2. Technical Specification of the LRB Tester

	Max. load (kN)	Max. Displacement (mm)	Max. Velocity
Vertical Capacity	30,000	150	1 (mm/sec)
Horizontal Capacity	±5000	±1,000	20 (mm/sec)
Moment Capacity	±500	±100	±1000 (kN.m)

Table 3. The Geometrical Specifications of LRB Isolator

Bearing diameter (mm)	Lead core diameter (mm)	Rubber thickness (mm)	No. of Rubber layers	Insert Plate Thickness (mm)	No. of Insert Plates	End Plate Thickness (mm)
1003	315	9.5	12	4	11	20

Table 4. LRB Mechanical Properties

Yield Stiffness K_u (kN/mm)	Post-Yield Stiffness K_d	Characteristic Strength (kN)	Equivalent damping ratio	Breaking Strain (mm)	Shear Load at Break (kN)
16.9	0.309	653.7	41.41%	244.6	705.1

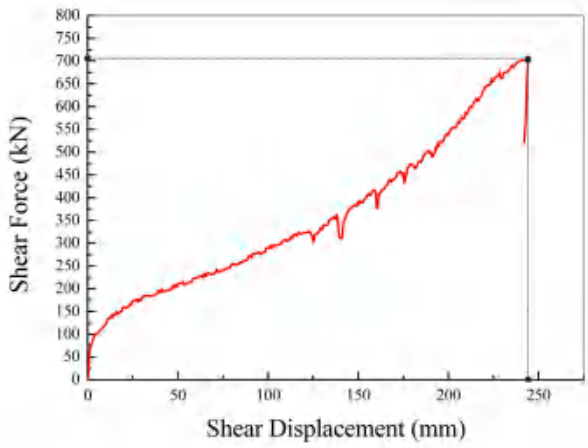

Fig. 4. Shear Load-displacement Curve

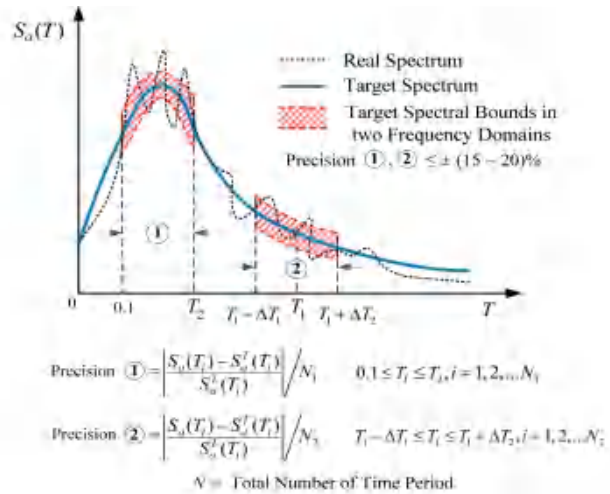

Fig. 5. Selection Analogy of Seismic Input Waves for Time History Analyses

In order to maintain the design in-plane pressure, a compressive load of 6600 KN was uniformly applied to the isolator, which was designed for the target shear strain of 1.5 with allowable displacement as 182 mm. For simplicity, a single bilinear zero-length element, clutched with the properties of eight isolators, was introduced into the finite element plant model. The geometrical specifications, stiffness and strength properties of each isolator, along with the ultimate shear capacity curve, are shown in tables 3 and 4, and Fig 4 respectively.

3. GROUND MOTION SELECTION

Long period structures like high-rise buildings and base-isolated NPPs tend to resonate for a relatively longer duration when struck by subduction zone earthquakes like Tohoku, which produced long-period and long duration ground motions. Hence, an attempt is being made to select the strong long period, as well as common ground motions out of the mega-event of Tohoku. In earthquake response analysis, the theory of response spectra is fundamentally involved where it further contributes to the design based methods for most of the seismic codes used worldwide. Referring to the study reported by Lee & Song (1999), an NPP is initially designed according to the response spectrum presented in United States Nuclear Regulatory Commission (USNRC) Reg. Guide 1.60 [12, 16]. Henceforth, the USNRC design spectrum is adopted as a target for the selection, considering the fact that earthquakes of Tohoku have evidently seemed to exceed all the current design standards and there is no design spectrum yet available to deal with such long-period time histories.

The selection of inputting seismic waves for the time history analyses is emphasized in two frequency domains. The first domain involves the flat region of the target spectrum which considerably involves the acceleration sensitive region, referring to the seismic effect on the high-order vibration modes of structures [16, 17]. The second domain corresponds to the natural period of the structure, referring to the seismic effect on the first vibration mode, which usually dominates the total seismic response of the structure. The selection analogy can be visualized in Figure 5 more clearly. The spectral compatibility between the

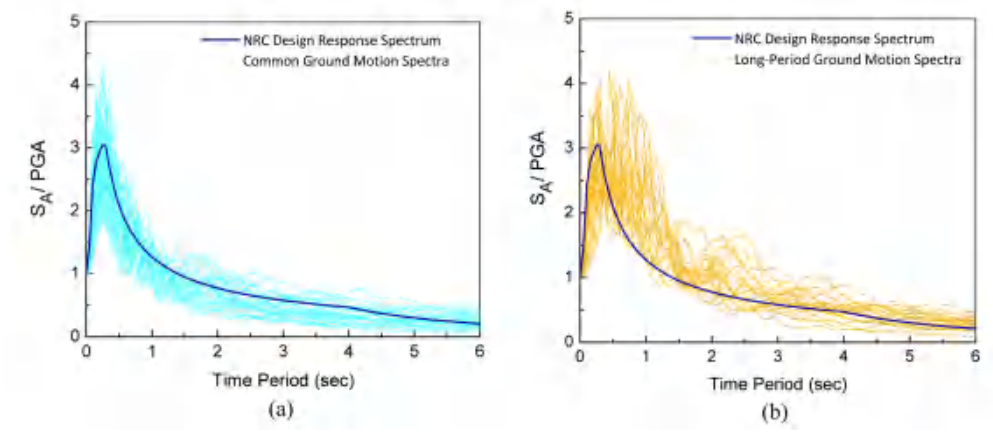

Fig. 6. NRC Spectral Comparison with (a) Common Ground Motions (b) Long-period Ground Motions

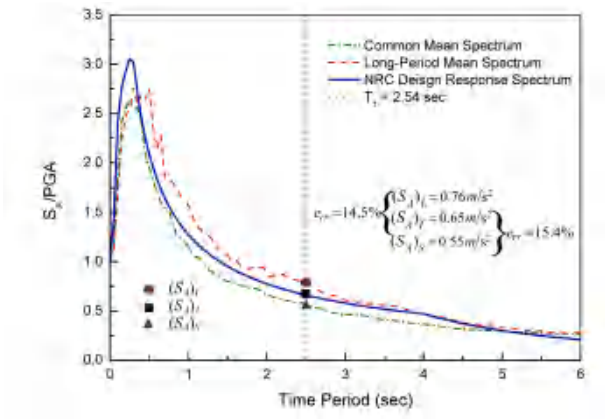

Fig. 7. Common & Long-period Mean Spectrum in Comparison with NRC Design Response Spectrum

target and selected ground motions is checked by dual frequency band method, in such a manner that the time histories which exceed the target spectrum, up to a precision of 15 to 20 %, are categorized as long-period motions, i.e. *Set A*. However, the common ground motions, i.e. *Set B*, are bound to lie equal or beneath the target spectrum with a threshold error of not more than 15 to 20% [18]. According to ASCE-7/10 16.1.3.1, the ground motions are scaled such that the average value of the 5% damped response spectra for the selected suite of ground motions should not be less than the 5% damped design response spectrum for periods ranging from 0.2T~1.5T, where T is the fundamental period of the structure being analyzed, i.e. 2.54 sec for the NPP, which is obtained by running an Eigen value analysis as a preceding step in performing the dynamic response analyses [19].

The application of the mentioned procedure is shown in Figure 6. It can be seen clearly in Figure 6(b) that the long period character is quite high, therefore for a more accurate selection, the first frequency domain is extended slightly beyond the flat region. Figure 7 demonstrates the comparative mean spectrum of the two types of ground motions, along with the spectral values and relative error err corresponding to the natural period of the NPP, hence exhibiting a successful selection of the ground motions.

4. SEISMIC RISK & HAZARD ANALYSIS OF NPP

4.1 Seismic Hazard

In the framework of PSHA, the rate and probability of exceedance of a certain earthquake intensity measure '*I*', e.g. PGA, at a site is computed by the expression derived by Baker [20]. Where $\lambda(I > x)$ refers to the frequency with which I exceeds a specified value *x*.

$$\lambda(I > x) = \sum_{i=1}^{n_s} \lambda(M_i > m_{\min}) \sum_{j=1}^{n_M} \sum_{k=1}^{n_R} P(I > x \mid m_j, r_k) P(M_i = m_j) P(R_i = r_k) \quad (1)$$

$\lambda(M_i > m_{\min})$ refers to the earthquake occurrence rate at source *i*. $P(I > x \mid m_j, r_k)$ is the probability of *x* exceeding *I* with magnitude m_j and distance r_k. $P(M_i = m_j)$ $P(R_i = r_k)$ represents the probability of an earthquake occurring with magnitude m_j at distance r_k. Moreover, n_s is the number of sources, n_M, n_R are the discretized intervals of magnitude and distance distributions (M_i, R_i) for source *i*, respectively.

The seismic source models for the Korean peninsula developed by Seo *et al*. and then presented by Nakajima *et al*. as source model A are considered for the seismic hazard analysis [21, 1]. The seismicity parameters of the model taken into account are shown in table 5. The attenuation relation of ground motions considered in the analysis and described by Baag *et al*. is abbreviated as follows:

$$\ln \mathrm{PGA}(\mathrm{cm/s^2}) = a_1 + a_2 M + a_3 \ln\left(\sqrt{R_{epi}^2 + a_0^2}\right) + a_4\left(\sqrt{R_{epi}^2 + a_0^2}\right) \quad (2)$$

Table 5. Seismic Source (Model A) Seismicity Parameters [1]

Source #	A	B	M_{min}	M_{max}
RS1	4.28	1.12	3.8	7.1
RS2	3.53	0.92	3.8	7.4
RS3	2.59	0.69	3.8	7.6
RS4	2.34	0.66	3.8	7.2
RS5	3.10	0.87	3.8	7.6
RS6	2.12	0.66	3.8	7.2
RS7	1.70	0.59	3.8	7.7

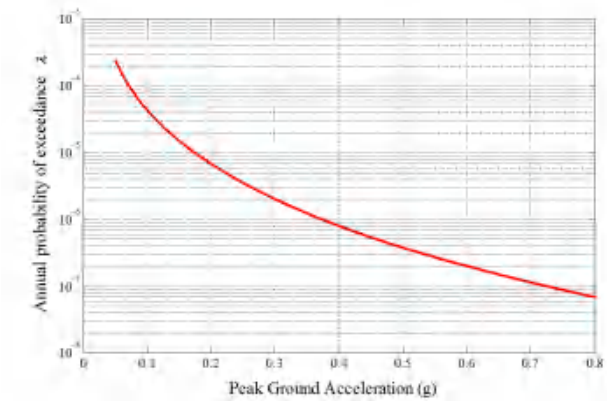

Fig. 8. Seismic 'PGA'Hazard Curve

Where a_1, a_2, a_3, a_4 and a_0 are 0.4, 1.2, -0.76, -0.0094 and 10 respectively, M is the local magnitude and R_{epi} is the epicentral distance in kilometers [22].

The factors A and B are the constants of the *Gutenberg-Richter recurrence* equation for the distribution of earthquake magnitudes in a particular region as follows, where λ_M denotes the rate of earthquakes with magnitudes greater than M [20, 23].

$$\log \lambda_M = A - B(M) \tag{3}$$

Hence, the estimated seismic hazard curve for PGA, summarizing the corresponding annual rate of exceeding intensity levels, is shown in Figure 8.

4.2 Fragility Estimation

A set of ground motions with noticeable long period content, along with the seismic signals of a common nature from the mega-event of the Tohoku earthquake, are chosen for the probabilistic seismic risk assessment of the base-isolated NPP reactor building. The selected ground motions are scaled with a PGA of 0.02g to 1.0g with an interval of 0.02g. The nonlinear time history analyses for the scaled motion inputs are then performed to find the

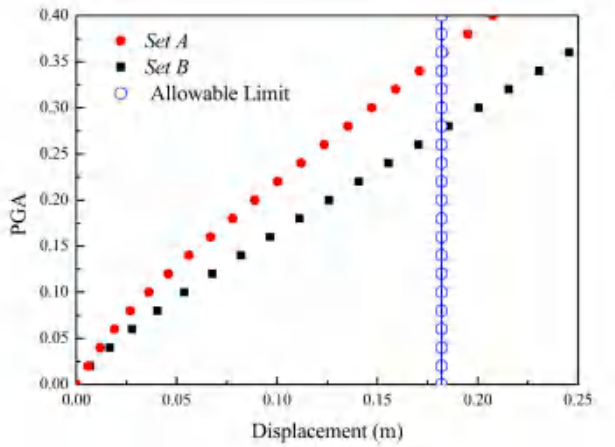

Fig. 9. Comparative displacement Response of the Isolated NPP

seismic response of the NPP. The maximum displacement exhibited by the base isolated node is captured as the prime response factor for the performance evaluation of the NPP. Figure 9 shows the comparative mean displacement responses for the two sets of ground motions scaled with different PGA's.

The conditional probability of NPP failure P_f is estimated by considering three state values as 0.5, 1.0 and 1.5 times the allowable isolator displacement D_D. The log-normal cumulative distribution function at each of these limit states is computed corresponding to the median capacity A_m and standard deviation β, which are taken in terms of the displacement exhibited by the isolated NPP relative to different PGAs, using the relation described by Zentner as follows;

$$P_f(a) = \int_0^a \frac{1}{x\beta\sqrt{2\pi}} e^{-0.5\left(\frac{\log(x/A_m)^2}{\beta^2}\right)} dx = \Phi\left(\ln\left(\frac{a}{A_m}\right)\Big/\beta\right) \tag{4}$$

Where $P_f(a)$ is the conditional probability of failure for a given value of a seismic input parameter, e.g. PGA, at any seismic motion level a. Φ(.) refers to the Normal or Gaussian cumulative distribution function [5]. The fragility curves for the two types of ground motions are shown in Figure 10, where State *I*, *II* and *III* refers to 0.5 × D_D, 1.0 × D_D and 1.5 × D_D, respectively.

It is well depicted that for *Set B* ground motions with long-period content, the probability of failure for all the limit state values is much higher than that of the *Set A* ground motions. The difference can be visualized as quite large, and therefore reflects the oppressive performance of the base isolated NPP and credibly higher level of seismic risk under the *Set B* seismic excitations. For the estimation of the probability distribution of each limit state value, the seismic hazard curve is adjoined by the fragility curves ($\lambda \times P_f$) of the base isolated NPP. From Figure 11, it can clearly be observed that the peak values in the probability

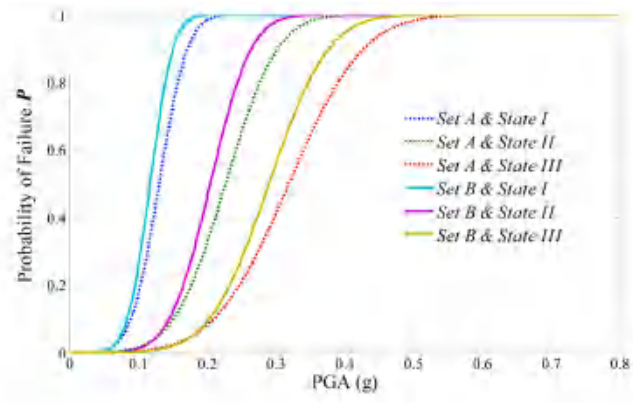

Fig. 10. Fragility Curves of the Base Isolated NPP

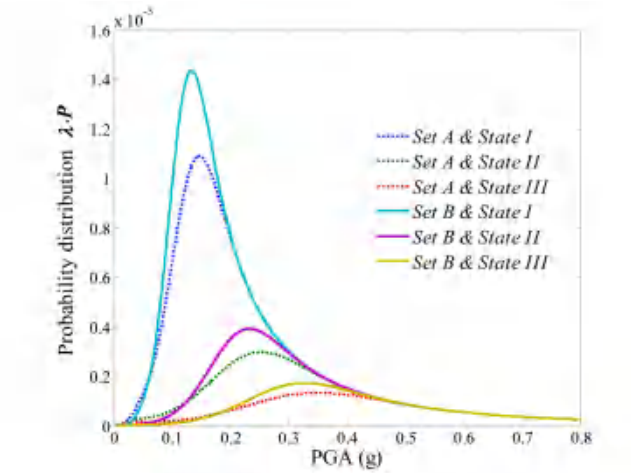

Fig. 11. Probability Distribution of the Limit State Values

distribution of States *I*, *II* and *III* of long-period ground motions stand higher as compared to the state values of *Set A*. Kim *et al*. named the term "dominant PGA", implying the PGA corresponding to the peak value of the probability distribution curve [24]. The dominant PGAs of long-period ground motions for all limit states are significantly smaller than the values under common ground motions, i.e. *Set A*.

Furthermore, the annual probabilities of the unacceptable performance corresponding to each of the limit states under both types of seismic motions are calculated. The approach described by Huang *et. al*, is considered as $\sum(\Delta\lambda_i \times (P_f)_i)$ for the computation of the annual probability values, where $\Delta\lambda_i$ is determined in *i*th intervals from the seismic hazard curve relative to the particular PGA of interest [25]. The plot of the results is clearly visualized in Figure 12. Once again, the analyses outcomes for *Set B* lie much higher than that of *Set A*. It can be seen that the annual probability of all the limit states under seismic excitations with a large long-period character is considerably larger. This implies the severity of the long-period content in a seismic signal referring to the unacceptable

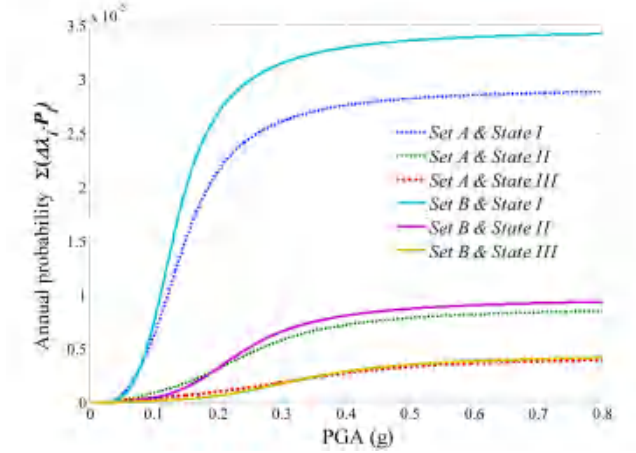

Fig. 12. Annual Probability of the Limit State Values

performance of the NPP. Hence, it signifies the need for a design spectrum encountering such effects for the safe design of nuclear facilities.

5. CONCLUSIONS

The study is initiated by the characterization and categorization of the seismic excitations of the Tohoku earthquake as common and long-period. This is achieved by providing a simplified criterion for selecting the input wave signals with the long-period content, as well as the signals of a common nature. The spectral compatibility of the selected ground motions is verified by the USNRC design spectrum. The 15 to 20 percent relative error is controlled in two frequency domains, which correspond to the flat range of the target response spectrum, as well as the natural period of the structure. If the error in these two frequency regions has exceeded the outer bounds of the USNRC spectrum, it signifies a higher long-period nature of the ground motion and is adopted as a long-period ground motion.

A probabilistic seismic risk analysis (PSRA) of the base-isolated NPP is conducted under selected real ground motions of the Tohoku event. The nonlinear analyses with the PGA range of 0.2g to 1.0g are performed, whereas the maximum displacement exhibited by the isolator is extracted as the prime response. The fragility curves are estimated by the simple log-normal method, in which three limit state values corresponding to allowable isolator displacements are considered to obtain fragility plots. It is found that the probability of failure of the NPP reactor building is much larger for long-period seismic motions. The seismic hazard curve is then combined with the fragility curves of each type of ground motion to obtain the probability distribution curves. The dominant PGAs in the probability distribution graph are quite small for the long-period motion, which indicates the severity and high

risk. Moreover, for annual probability, results for *Set A* are observed as credibly smaller than that of strong long-period excitations.

Hence, for *Set B*, the overall response of the base-isolated NPP is seen to be much amplified as compared to *Set A*. It shows the efficient selection of the common and long-period ground motions of the Tohoku earthquake. In addition, it can be inferred that ground motions with a longer time history and long-period wave component can cause severe damage and hazards to the NPP and other nuclear facilities. This fact necessitates the careful classification and selection of ground motions for seismic risk assessment of NPP which can expose the stronger effects of long-period components of earthquakes. As the results have clearly shown the severities of the long-period content in a seismic signal, so a design spectrum encountering such effects for the safe design of nuclear facilities is importantly required. Under the conditions presented, the long-period property, spatial variation, non-stationarity of seismic signals, and pertinent effects on base-isolated NPP considering soil-structure interaction will be the direction of future research to provide more coherent outcomes with significant applications for nuclear facilities in Korea and around the world.

ACKNOWLEDGEMENTS

This work was supported by the Nuclear power Core Technology Development Program of the Korea Institute of Energy Technology Evaluation and Planning (KETEP) grant financial resource from the Ministry of Trade, Industry & Energy, Republic of Korea (No. 2011151010010B)

REFERENCES

[1] Nakajima M, Choi I-K, Ohtori Y, Choun YS. Evaluation of seismic hazard curves and scenario earthquakes for Korean sites based on probabilistic seismic hazard analysis. *Nuclear Engineering and Design* 2007; **237**: 277-288.

[2] Choi I-K, Nakajima M, Choun YS, Ohtori Y. Development of the site-specific uniform hazard spectra for Korean nuclear power plant sites. *Nuclear Engineering and Design* 2009; **239**: 790-799.

[3] Kennedy RP, Cornell CA, Campbell RD, Kaplan S. and Perla HF. Probabilistic Seismic Safety of An Existing Nuclear Power Plant. *Nuclear Engineering and Design* 1980; **59**: 315–338.

[4] Kennedy RP and Ravindra MK. Seismic Fragilities for Nuclear Power Plant Risk Studies. *Nuclear Engineering and Design* 1984; **79**: 47–68.

[5] Zentner I. Numerical computation of fragility curves for NPP equipment. *Nuclear Engineering and Design* 2010; **240**: 1614-1621.

[6] Pisharady AS, Basu PC. Methods to derive seismic fragility of NPP components: A summary. *Nuclear Engineering and Design* 2010; **240**: 3878-3887.

[7] Furumura T, Takemura S, Noguchi S, Takemoto T, Maeda T, Iwai K, Padhy S. Strong ground motions from the 2011 off-the Pacific-Coast-of-Tohoku, Japan (Mw=9.0) earthquake obtained from a dense nationwide seismic network, *Landslides* 2011; **8**: 333-338.

[8] Takewaki I. Preliminary Report of the 2011 off the Pacific Coast of Tohoku Earthquake, *J. Zhejiang Univ-Sci. A (Appl Phys & Eng)* 2011; **12** (5): 327-334.

[9] Takewaki I, Murakami S, Fujita K, Yoshitomi S. and Tsuji M. (2011). The 2011 off the Pacific Coast of Tohoku Earthquake and Response of High-Rise Buildings under Long-Period Ground Motions, *Soil Dynamics and Earthquake Engineering* 2011; **31**: 1511-1528.

[10] Xiang Z. and Li Y. Statistical Characteristics of Long Period Response Spectra of Earthquake Ground Motion. *12th World Conference on Earthquake Engineering* 2000; Auckland, New Zealand, 12WCEE, January.

[11] McKenna F, Fenves GL. OpenSees, the open system for earthquake engineering simulation 2001. http://opensees.berkeley.edu

[12] Lee NH, Song KB. Seismic Capacity Evaluation of the Prestressed/Reinforced Concrete Containment, Young-Gwang nuclear power plant units 5 & 6. *Nuclear Engineering and Design* 1999; **192**: 189-203.

[13] Korea Testing & Research Institue. Lead Rubber Bearing (LRB) Performance Evaluation. KTIR 2011. 11-TBS-140.

[14] Naeim F, Kelly JM. Design of Seismic Isolated Structures: from theory to practice, *John Wiley and Sons*, *Inc*., New York, USA, 1999; 63-76.

[15] International Standard. Elastomeric seismic-protection, Part1: Test methods, *ISO 22762:2010*, *6.2.2*, Geneva, Switzerland, 2010; 20-26.

[16] Regulatory Guide 1.60. Design Response Spectra for Seismic Design of Nuclear Power Plants, *U.S. Nuclear Regulatory Commission*, Washington, DC, 1973.

[17] Kalkan E, Chopra AK. Practical guidelines to select and scale earthquake records for nonlinear response history analysis of structure, *U.S. Geological Survey, Earthquake Engineering Research Institute*, 2010.

[18] Yang P, Li YM, Lai M. A New Method for Selecting Input Waves for Time History Analysis. *China Civil Engineering Journal* 2000; **33** (6): 33-37.

[19] American Society of Civil Engineers. Minimum Design Loads for Buildings and Other Structures, ASCE Standard (ASCE/SEI 7-10). 2010.

[20] Baker JW. (2008). An Introduction to Probabilistic Seismic Hazard Analysis (PSHA). *White Paper* 2008; Version 1.3: 72 pp.

[21] Seo JM, Min, GS, Choun YS, Choi I-K. Reduction of Uncertainities in Probabilistic Seismic Hazard Analysis. *KAERI/CR-65* 1999.

[22] Baag CE, Chang SJ, Jo ND. and Shin JS. Evaluation of seismic hazard in the southern part of Korea. *The Second International Symposium on Seismic Hazards and Ground Motion in the Region of Moderate Seismicity* 1998.

[23] Gutenberg, B., and Richter, C. F. Frequency of earthquakes in California. *Bulletin of the Seismological Society of America* 1944; **34**(4): 185-188.

[24] Kim DK, Cho SG. and Dong YF. Generation of Non-Stationary Ground Motions for Probabilistic Seismic Risk Analysis of Nuclear Power Plants. *15th World Conference on Earthquake Engineering* 2012, Lisboa, Portugal, 15WCEE.

[25] Huang YN, Whittaker AS, Luco N. Seismic Performance Assessment of Base-Isolated Safety-Related Nuclear Structures, *Earthquake Engineering and Structural Dynamics* 2010; **39**(13): 1421-1442